Preparative and Structural Chemistry of Chiral P,N-Bidentate Complexes of Palladium(II) and Platinum(II)

Alberto Albinati,*,† Francesca Lianza,† Heinrich Berger,‡ Paul S. Pregosin,*,‡ Heinz Rüegger,‡ and Roland W. Kunz§

Institute of Chemical Pharmacy, University of Milan, 20131 Milano, Italy, Institute of Inorganic Chemistry, ETH-Zentrum, 8092 Zürich, Switzerland, and Department of Organic Chemistry, University of Zürich, 8057 Zürich, Switzerland

Received June 1, 1992

The preparations of the valine-derived chiral (L) P,N-bidentate ligand $(p\text{-}CH_3C_6H_4)_2PCH_2CH(Pr^i)NHCH_2(p\text{-}OCH_3C_6H_4)$ (**1**), the complexes $PdCl_2$(**1**) (**2**) and $PtCl_2$(**1**) (**3**), and the deprotonated dimeric compound $[Pt(1-H)Cl]_2$ (**4**), as well as the iodo analog of **3**, are reported. The solid-state structure of **2** has been determined by X-ray diffraction and shown to contain a five-membered metal chelate in which the *N*-benzyl and Pr^i groups are equatorial, whereas the solution-state structure, determined by using one- and two-dimensional ^{1}H-NMR methods, is shown to have both of these groups pseudoaxial. The results are discussed with the help of molecular mechanics calculations and solid-state ^{31}P-NMR methods. ^{1}H, ^{13}C, ^{15}N, and ^{31}P results are reported. Crystals of **2**·0.5$CHCl_3$ are orthorhombic, of space group $P2_12_12_1$, with a = 13.230 (4) Å, b = 17.133 (9) Å, c = 25.877 (8) Å, Z = 8, and V = 5865 (3) Å^3.

Introduction

It is now well-known[1-6] that optically active chelating ligands create a pocket which can transfer the chirality to developing stereogenic centers in the course of a reaction, e.g. asymmetric hydrogenation.[1] It is not absolutely necessary that the chelate be frozen into a specific conformation,[2] although this is often the case for five-membered rings containing substituents in the backbone[3] or for binaphthyl chelate ligands,[4] where free rotation is not permitted.

The decision as to the structure of such "pockets" has often been derived from X-ray results, which did, indeed, show a chiral array of phenyl groups when two different $-PPh_2$ groups were used as the end fragments of the chelating ligand; however, a solution structure which differs from that of the solid state and/or a case where the reactive diastereomer has a different structure than that observed in the ground state is certainly conceivable.[6]

We have recently begun to study three-dimensional structural aspects of dissolved metal complexes using Overhauser effects and, specifically, 2-D NOESY methods.[7-10] Our efforts have been centered around palladium(II) allyl chemistry, and we were able to (a) distinguish subtle structural differences in diastereomers of a Pd[II]BINAP complex[8] and (b) locate C–H bonds which are proximate to transition metal centers in square planar environments.[7,10] Our approach has been based on the ability to assign key "reporter"[7] protons, e.g., the ortho protons of the BINAP-PPh_2 groups, and then use NOE's from these to make structural assignments. In several cases we have optimized the NOE work with the help of some simple calculations.[8]

In all of these molecules the proton spectra were frequently moderately complicated, with the result that a substantial effort was required in assigning spectra before the structural information became available. To reduce this aspect of the problem, we have prepared the ligand **1**, using the commercially available chiral

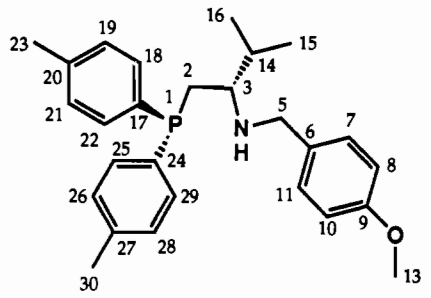

1

amino acid L-valine, as shown in Scheme I. Compound **1** has the advantage of specifically chosen para substituents which allow a ready assignment of the various aryl protons via simplification of their spin systems while adding easily assignable additional NOE probes. In addition, we can now prepare chiral complexes containing both relatively weak and relatively strong donors and consider the effects of these electronic changes on a variety of chemical transformations. A variety of chiral P,N-ligands have been prepared and utilized previously by Hayashi and coworkers.[11] Moreover, bidentate P,N-ligand and their complexes have been reported by several groups.[12-14] We report here our initial NMR spectroscopic results for complexes **2**–**4** combined

† University of Milan.
‡ ETH Zurich.
§ University of Zürich.

(1) Knowles, W. S. *Acc. Chem. Res.* **1983**, *16*, 106. Merrill, R. E., *Chem. Tech.* **1981**, *11*, 118.
(2) Fryzuk, M. D.; Bosnich, B. *J. Am. Chem. Soc.* **1977**, *99*, 6262.
(3) Noyori, R.; Kitamura, M. In *Modern Synthetic Methods*; Scheffold, R., Ed.; Springer Verlag: Berlin, 1989; Vol. 5.
(4) Noyori, R. *Chem. Br.* **1989**, 883.
(5) Vineyard, B. D.; Knowles, W. S.; Sabacky, M. J.; Bachmann, G. L.; Weinkauff, D. J. *J. Am. Chem. Soc.* **1977**, *95*, 5946.
(6) Brown, J. M. *Chem. Br.* **1989**, 276. Halpern, J.; Landis, C. R. *J. Am. Chem. Soc.* **1987**, *109*, 1746.
(7) Albinati, A.; Ammann, C.; Pregosin, P. S.; Rüegger, H. *Organometallics* **1990**, *9*, 1826. Albinati, A.; Kunz, R. W.; Ammann, C. J.; Pregosin, P. S. *Organometallics* **1991**, *10*, 1800.
(8) Rüegger, H.; Kunz, R. W.; Ammann, C. J.; Pregosin, P. S. *Magn. Reson. Chem.* **1991**, *29*, 197. Ammann, C.; Pregosin, P. S.; Rüegger, H.; Albinati, A.; Lianza, F.; Kunz, R. W. *J. Organomet. Chem.* **1992**, *423*, 415.
(9) Pregosin, P. S.; Wombacher, F. *Magn. Reson. Chem.* **1991**, *29*, 9106.
(10) Togni, A.; Blumer, R. E.; Pregosin, P. S. *Helv. Chim. Acta* **1991**, *74*, 1533. Togni, A.; Rihs, G.; Pregosin, P. S.; Ammann, C. *Helv. Chim. Acta* **1990**, *73*, 723.
(11) Hayashi, T.; Konishi, M.; Fukushima, M.; Kanehira, K.; Hioki, T.; Kumada, M. *J. Org. Chem.* **1983**, *48*, 2195.
(12) Taqui Khan, M. M.; Reddy, V. V. S.; Bajaj, H. C. *Inorg. Chim. Acta* **1987**, *130*, 163.
(13) Farnetti, E.; Nardin, G.; Graziani, M. *J. Chem. Soc., Chem. Commun.* **1988**, 1264.

0020-1669/93/1332-0478$04.00/0

Scheme I. Synthesis of Ligand 1

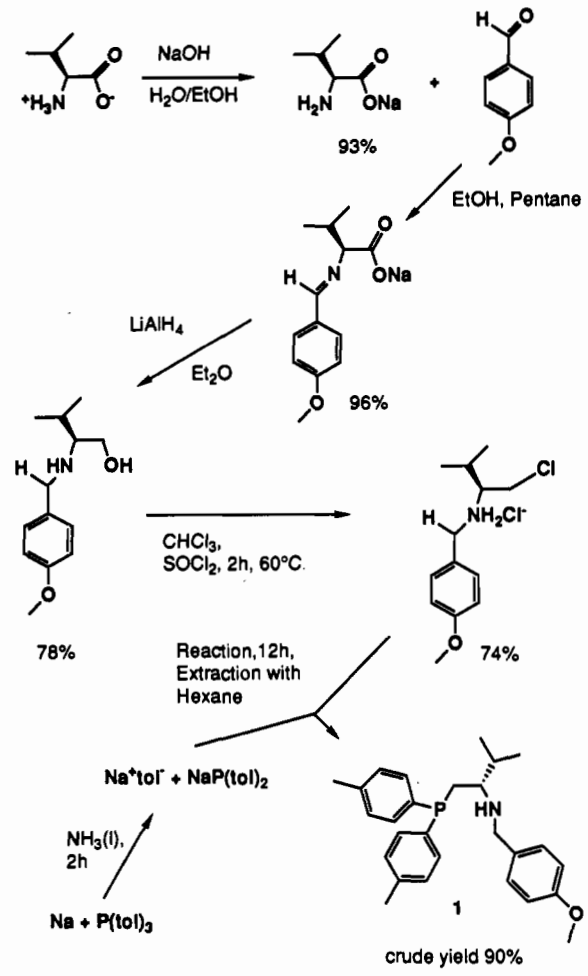

with the solid-state structure for $PdCl_2$(1) (**2**) determined by X-ray diffraction plus some calculations concerned with the relative stability of various conformers of **2**.

Results and Discussion

As shown in Scheme I, the new ligand can be prepared via condensation of the amino acid to a Schiff base followed by reduction to the amino alcohol using $LiAlH_4$. Conversion of the alcohol to the chloride, followed by reaction with the PPh_2 anion gave the product. We were concerned that racemization might occur during the hydride reduction, as $LiAlH_4$ is potentially basic. Consequently, we have prepared our new amino alcohol via a second method in which, initially, L-valinol (which is commercially available) is condensed with *p*-methoxybenzaldehyde and the resulting imine reduced with hydrogen (Pd/charcoal). In both syntheses we find the same optical rotation after workup, so that the hydride route seems reasonable.

Scheme II shows the route to complexes **2**–**4**. Complexes **2** and **3** were prepared using relatively labile starting materials to promote chelate formation, and the complexes were characterized via microanalytical, FAB mass spectral, IR, and multinuclear NMR measurements. The FAB mass spectra for **2** and **3** show an intense group of peaks at an *m/e* corresponding to the fragment [molecular ion – Cl]$^+$; in our experience this is typical for palladium, platinum, and even mercury dichloro complexes.[15] Complexes **2** and **3** also show the two IR vibrations expected for the symmetric and asymmetric M–Cl stretches: 332, 270 cm^{-1} and 331, 288 cm^{-1}, respectively, and there are N–H vibrations

(14) Park, S.; Hedden, D.; Rheingold, A. L.; Roundhill, D. M. *Organometallics* **1986**, *5*, 336, 1305.
(15) Pregosin, P. S. Unpublished results.

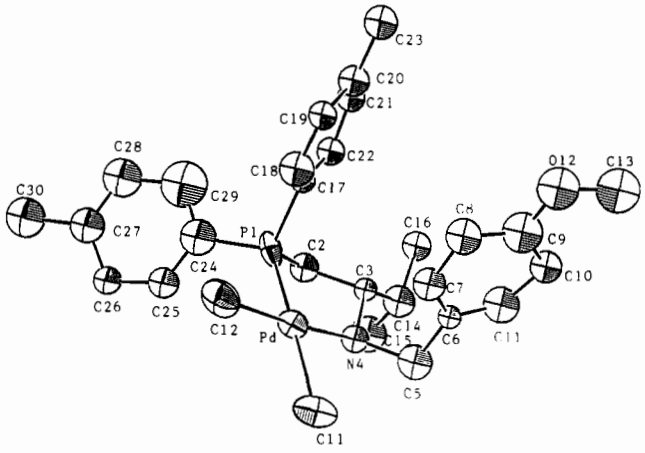

Figure 1. ORTEP view of one of the molecules of **2**.

Scheme II. Synthesis of Pt– and Pd–Dichloro Complexes

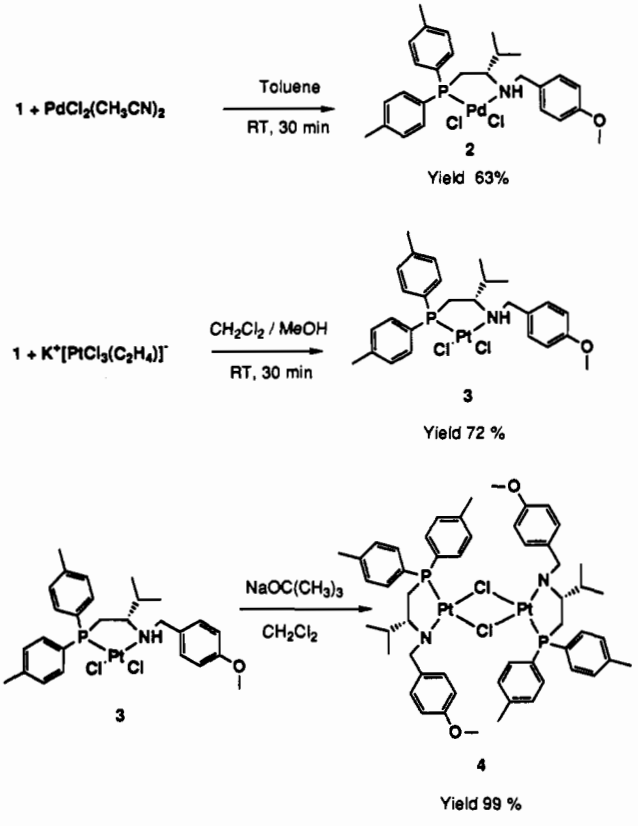

at 3111 and 3263 cm^{-1}, respectively. The Pt–Cl stretches in **4** do not appear in the region 300–400 cm^{-1}, thereby supporting a halogen-bridged structure. Analytical data for the complexes are given in the Experimental Section.

X-ray Structure of 2. As ligand **1** is new, we decided to determine the solid-state structure of some of its complexes because these data could serve as models for the NOESY results. The structure of the palladium complex **2** reveals two independent molecules in the unit cell, and one of these is shown in an ORTEP plot in Figure 1. Solid-state ^{31}P-NMR shows that these molecules exist in the crude product as well. Since the two forms are very similar, we discuss the structure in terms of an average of the two, although Table I gives bond lengths and bond angles for both molecules.

Complex **2** has, as expected, a distorted square planar geometry at palladium. The two Pd–Cl lengths are comparable in both molecules, with that trans to P, 2.38 (1) Å, somewhat longer than that trans to N, 2.30 (1) Å, due to the larger trans influence of

Table I. Selected Bond Lengths (Å) and Bond Angles (deg) for **2**

	molecule 1	molecule 2
Pd–Cl(1)	2.36 (1)	2.39 (1)
Pd–Cl(2)	2.31 (1)	2.28 (1)
Pd–P(1)	2.19 (1)	2.18 (1)
Pd–N(4)	2.16 (3)	2.12 (3)
P(1)–C(2)	1.83 (4)	1.75 (4)
N(4)–C(3)	1.50 (4)	1.57 (5)
C(2)–C(3)	1.53 (5)	1.52 (5)
P(1)–C(17)	1.79 (4)	1.81 (3)
P(1)–C(24)	1.74 (4)	1.77 (3)
N(4)–C(5)	1.51 (5)	1.59 (4)
C(3)–C(14)	1.58 (5)	1.53 (5)
C(5)–C(6)	1.46 (5)	1.53 (5)
Cl(1)–Pd–P(1)	178.3 (4)	177.0 (4)
Cl(2)–Pd–N(4)	174.5 (8)	173.6 (8)
Cl(1)–Pd–N(4)	95.4 (8)	92.1 (8)
Cl(1)–Pd–Cl(2)	90.1 (4)	92.8 (4)
Cl(2)–Pd–P(1)	90.1 (4)	89.1 (4)
P(1)–Pd–N(4)	84.4 (8)	85.8 (7)
Pd–P(1)–C(2)	102 (1)	103 (1)
Pd–N(4)–C(3)	111 (2)	111 (2)
P(1)–C(2)–C(3)	103 (2)	109 (3)
N(4)–C(3)–C(2)	107 (3)	108 (3)
C(3)–N(4)–C(5)	110 (3)	111 (2)
C(17)–P(1)–C(24)	109 (2)	104 (2)

a tertiary phosphine relative to that of an amine.[16] The Pd–P distance is relatively short[17] at 2.18 (1) Å and is reasonable for P trans to Cl; however, the Pd–N distance is rather long, 2.14 (3) Å, but not unprecedented.[17,18] The Cl–Pd–Cl angle at 91.4 (5)° and the Cl(1)–Pd–N angle at 93.7 (8)° reveal only minor distortions from the ideal value as do the trans angles P–Pd–Cl(1) and N–Pd–Cl(2) of 177.6 (5) and 174.0 (8)°, respectively. The chelate angle P–Pd–N of 85.1 (8)° is normal for such a five-membered ring[17] and is presumably related to the slightly larger than 90° angles noted above. Cross et al.[19] have determined the solid-state structures for the P,N–palladium(II) complexes $PdCl_2[Ph_2PCH_2CH((CH_2)_nSMe)NMe_2]$, $n = 2, 3$, in which the sulfur ligand is not coordinated, and found similar bond lengths and bond angles. In summary, the immediate coordination sphere for **2** shows no special features apart from the somewhat short Pd–P and the somewhat long Pd–N bonds. If one defines a coordination plane using the palladium and the two halogens, then the phosphorus atoms (in both molecules) are ca. 0.10 Å from the plane and the nitrogen atoms are, in one case, ca. 0.03 Å away and, in the second molecule, ca. 0.21 Å away, both in the same direction as the phosphorus atoms.

The arrangement of the substituents on carbon, nitrogen, and phosphorus is interesting, and we view these orientations by considering the best plane derived from the five-membered chelate ring. The valine isopropyl group is pseudoequatorial as judged by the fact that the Pr^i methine carbon, C(14), is only on average ca. 0.05 (3) Å from this plane whereas the benzyl carbon, C(5), is ca. 0.55 (3) Å from this plane, somewhat more equatorial than axial. The axial phosphorus phenyl carbon, C(17), is ca. 1.88 (4) Å off the plane and is on the same side as the benzyl phenyl group. The corresponding equatorial phosphorus carbon, C(24), is ca. 0.80 (3) Å from the plane. Overall, the best description of the position of the Pr^i and Bz groups seems to be both equatorial with the PPh_2 group having one phenyl axial lying on the same side as the benzyl group.

NMR Spectroscopy. An analytically pure sample of **2** shows a relatively simple proton spectrum at 500 MHz indicative of primarily one species. This is not necessarily to be expected since the nitrogen is a stereogenic center and coordination could afford isomers. Moreover, the ^{31}P-NMR spectrum shows only a single line at both ambient probe temperature and 210 K. The NH proton, at ca. 5 ppm, shows (very different) spin–spin couplings to both the benzyl protons, suggesting that the nitrogen is coordinated. An uncoordinated secondary amine (if it were long-lived) would result in loss of these spin–spin interactions. These points combined with the crystallographic data (one would expect a different space group if both diastereomers were present in equal amounts) suggest that we are dealing with one diastereomer; however, we cannot rigorously exclude the presence of two rapidly exchanging diastereomers in solution. The presence of predominantly one isomer, combined with the simplicity deliberately built into **1** in terms of understanding its ^{1}H spectra, readily allows a complete assignment of both the low- and high-field regions. Figure 2 shows an expansion of the region between 2.0 and 2.8 ppm, which reveals the chelate PCH_2CHN ring protons, the nonequivalent *p*-tolyl methyls, and the CH of the Pr^i group. Note that there is a relatively large ^3J(P,H) coupling constant indicated, ca. 32.4 Hz, and that this value has been confirmed via an inverse phosphorus–proton INEPT spectrum. The magnitude of this vicinal coupling is known[20] to be a function of the P–C–C–H dihedral angle and suggests this angle in **2** to be ca. 150°. This observation, in itself, strongly suggests the presence of a pseudoaxial Pr^i group.

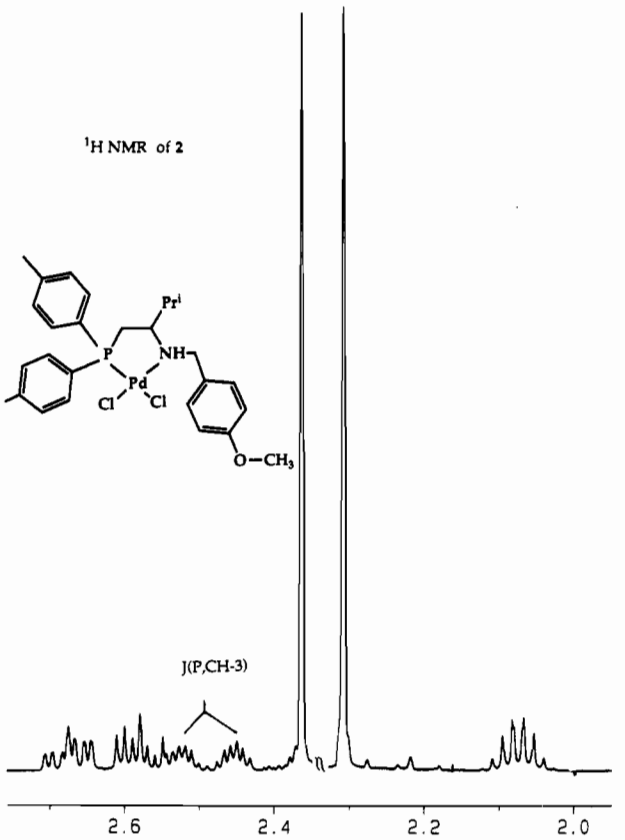

Figure 2. Section of the 500-MHz ^{1}H-NMR spectrum of **2** showing the PCH_2CH protons and the large ^{31}P coupling to H(3).

Figure 3 reveals an expansion of the aromatic region and indicates the ortho protons of the two nonequivalent phosphorus *p*-tolyl rings, and this brings us to the NOESY measurements.

A section of the 2-D NOESY spectrum for **2** at 500 MHz is shown in Figure 4. There are a number of interesting cross-peaks which allow us to conclude that (1) one of the two

(16) Palenik, G. J.; Giordano, T. J. *J. Chem. Soc., Dalton Trans.* **1987**, 1175. Wisner, J. M.; Borczak, T. J.; Ibecs, J. A. *Organometallics* **1986**, *5*, 2044. Albinati, A.; Lianza, F.; Berger, H.; Pregosin, P. S. *Inorg. Chim. Acta* **1992**, *200*, 771.
(17) Orpen, A. G.; Brammer, L.; Allen, F. H.; Kennard, O.; Watson, D. G.; Taylor, R. *J. Chem. Soc., Dalton Trans.* **1989**, S1.
(18) Albinati, A.; Arz, C.; Pregosin, P. S. *Inorg. Chem.* **1987**, *26*, 508.
(19) Cross, G.; Vriesema, B. K.; Boven, G.; Kellog, R. M.; van Bolhuis, F. *J. Organomet. Chem.* **1989**, *370*, 357.
(20) Bentrude, W. G.; Setzer, W. N. In *Methods in Stereochemical Analysis*; Verkade, J. G., Quin, L. D., Eds.; VCH Publishers: New York, 1987; Vol. 8, p 365 and references therein.

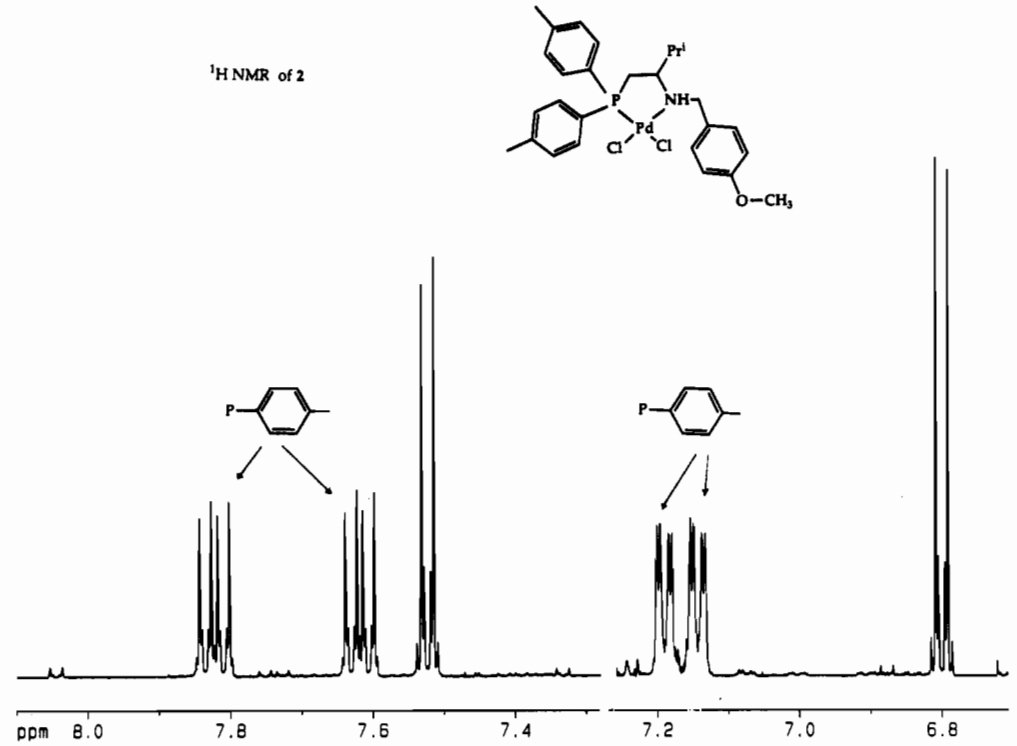

Figure 3. Section of the 500-MHz ^{1}H-NMR spectrum of **2** showing the aromatic protons for the P(*p*-Tol)$_2$ and NCH$_2$(*p*-CH$_3$OC$_6$H$_4$) moieties. The two low-field absorptions stem from the nonequivalent ortho protons of the P(*p*-Tol) groups.

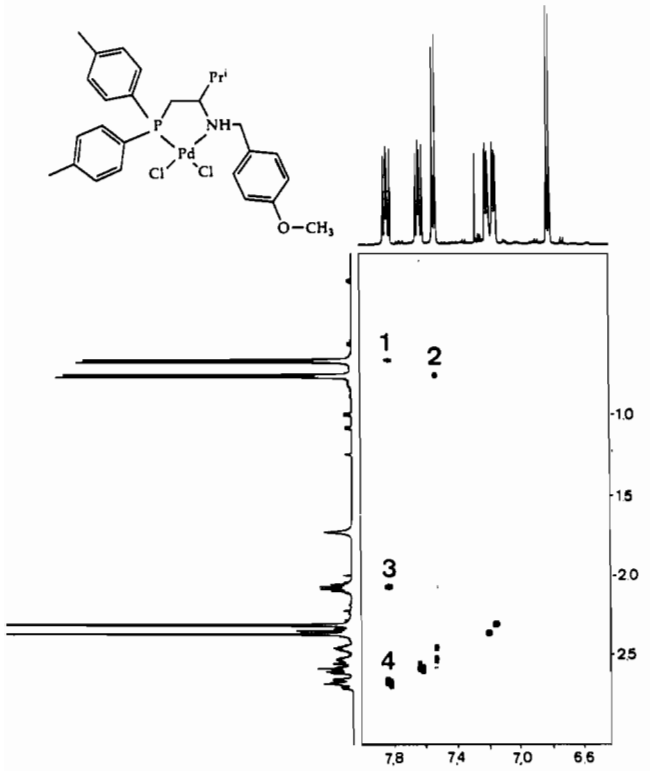

Figure 4. Section of the 500-MHz ^{1}H 2-D NOESY spectrum for **2**, showing important cross-peaks. Note that the two Pr^i methyl groups recognize completely different "sides" of the complex: cross-peak 1 from one Pr^i CH$_3$ to the P(*p*-Tol); cross-peak 2 from the other Pr^i CH$_3$ to the Bz protons; cross-peaks 3 and 4 from an Pr^i CH$_3$ to the Pr^i CH and one of the two PCH$_2$ protons, respectively.

nonequivalent Pr^i methyl groups is close to one of the P(*p*-Tol) ring ortho protons, (2) the CH of the Pr^i is relatively close to the same ortho protons of one of the P(*p*-Tol) rings as in point 1, (3) the other Pr^i methyl sees the ortho protons of the benzyl ring, and (4) one of the PCH$_2$ protons is relatively close to one of the NCH$_2$(*p*-CH$_3$OC$_6$H$_4$) protons.

There are several important structural conclusions which can be drawn from the presence of these observed cross-peaks, but the main point concerns the placement of the Pr^i group in that from points 1 to 3 it must be axial. Together with point 4, we conclude that we have a conformation in which both the Pr^i and benzyl become axial; this structure is shown in Figure 5, presented later on, in connection with the calculations. It is not possible to rationalize these solution-state NOE results—and that for the three-bond P,H coupling mentioned above—using the structure found in the solid state. There are a number of other interesting structural features which one can derive, e.g. the rotation of Pr^i is obviously not completely free; however, these are of secondary importance. We have also recorded ^{13}C and ^{31}P (solution and solid-state) spectra for **2** and **3** and determined $^1J(^{15}N,H)$ of the coordinated secondary amine using heteronuclear multiple-quantum methods. These latter values, 71.7 and 73.3 Hz, for **2** and **3**, respectively, are consistent with approximate sp^3 hybridization at nitrogen.[21,22] Our interest in the ^{31}P solid-state measurement arose from the possibility that the powder might exist in two diastereomeric forms. In the solid-state we observe two ^{31}P resonances with approximately equal intensities separated by ca. 4.4 ppm. The chemical shift difference is, unfortunately, consistent either with nonequivalent molecules in the unit cell or with diastereomers.[23,24] As we know from the crystallography that the former situation exists, we are inclined to believe that the solid, just as the solution, shows essentially a single diastereomer. At 210 K in CD_2Cl_2 we find only one phosphorus resonance.

The NMR spectroscopy for the platinum analog, **3**, is similar to that for **2** in many ways, except that one also observes the satellites due to the presence of spin–spin coupling to the ~33.7% abundant ^{195}Pt. This metal–ligand coupling is useful; e.g., in the

(21) Witanoski, M.; Styaniak, L.; Webb, G. A. *Annu. Rep. NMR Spectrosc.* **1981**, *11B*.
(22) Axenrod, T.; Pregosin, P. S.; Wieder, M. J.; Becker, E. D.; Bradley, R. B.; Milne, G. W. A. *J. Am. Chem. Soc.* **1971**, *93*, 6536.
(23) Rahn, J.; Baltusis, L.; Nelson, J. H. *Inorg. Chem.* **1990**, *29*, 750.
(24) Davis, J. A.; Dutreme, S.; Pinkerton, A. A. *Inorg. Chem.* **1991**, *30*, 2380.

Table II. ^{1}H-NMR Data for **2** and **3**

signal	multiplicity, δ, J	
	2	**3**
H–C(2)	m, 2.58, ^2J(P,H) = 11.3 Hz[a]	m, 2.53, ^2J(P,H) = 11.8 Hz[a]
	m, 2.68[b]	m, 2.63[b]
H–C(3)	m, 2.42, ^3J(P,H) = 34.2 Hz[a]	m, 2.34, ^3J(P,H) = 36.4 Hz[a]
	m, 2.53	
NH	s, 5.29[c]	d, 4.74
H–C(5)	m, 4.27	m, 3.72
	m, 4.43	d, 4.78
H–C(&,11)	m, 7.52	m, 7.36
H–C(8,10)	m, 6.80	m, 6.85
OCH_3	s, 3.77	s, 3.78
H–C(14)	m, 2.07	m, 1.96
CH_3	d, 0.67[b]	d, 0.48[b]
	d, 0.76	d, 0.63
H–C(18,22)	m, 7.62	m, 7.73
H–C(19,21)	m, 7.19	m, 7.20
H–C(23)	s, 2.36	s, 2.35
H–C(25,29)	m, 7.82	m, 7.97
H–C(26,28)	m, 7.14	m, 7.22
H–C(30)	s, 2.31	s, 2.35

[a] The P,H coupling was determined via ^{31}P-^{1}H-retro-INEPT. [b] On the same side as the phenyl protons H–C(25) and H–C(29), which lie on the same side as the Pr^i group; 0.67 CH_3 shows NOE to H–C(25) and H–C(29). [c] Broad signal.

^{31}P spectrum we find ^1J(Pt,P) = 4040 Hz, and this is consistent[25,26] with the cis orientation suggested by the IR data. Both the solution and solid-state ^{31}P spectra reveal only one complex. The ^{1}H NOESY spectrum for **3** shows the same important NOE's as described above for **2**, and if anything, the quality of the data is better. The large ^3J(P,H) coupling is observable via the NOESY cross-peaks (the 1-D spectrum shows considerable overlap of these signals with the tolyl CH_3's), and the ^3J(NH,CH_2) coupling is present and once again selective, i.e., larger to one of the benzyl protons than to the other. In summary, **3** has the same structure as **2**, so that further discussion is not necessary.

The preparation of **4** involves precipitation of NaCl, and this observation combined with the microanalytical and NMR results strongly pointed to a dimeric material. Moreover, X-ray fluorescence results confirm the Pt:P:Cl ratio to be ca. 1:1:1; however, the decision as to which of the following two structures (I and II) was correct was made primarily on the basis of the IR data in the region 300–400 cm^{-1}.

I

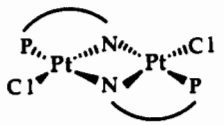

II

We do not find bands attributable to a Pt–Cl stretch in this region[27] and so favor I over II. Naturally, the N–H stretch, readily observed in **2** and **3**, is absent in **4**. In some respects the ^{31}P-NMR spectrum for **4** was not as helpful as hoped, in that ^1J(Pt,P) at 3688 Hz is not especially diagnostic, although this value is certainly consistent with I.

We note that (a) the iodo analog of **3**, complex **5**, was prepared and (b) **4** reacts with HCl to yield **3** in good yield. Selected NMR data for complexes **2**–**5** can be found in Tables II–IV and the Experimental Section.

Calculations. The obvious lack of agreement between the solution and solid-state results with respect to the conformation of our five-membered ring has prompted us to consider some calculations in the hope of gaining further insight. To this end, we have utilized Allinger's new force field program MM3.[28a] The missing parameters around palladium in the five-membered chelate were derived on the basis of the structure reported in this publication as well as two available structures from the Cambridge Crystallographic Database (VASGAX, VASFOK). The input parameter file and the MM3 structure input files are available as supplementary material from the authors.

The stereogenic carbon in the five-membered ring is *S* as introduced by the starting material; however, the coordinated nitrogen represents a second stereogenic center and is of unknown stereochemistry. Therefore, both the *SS* and the *SR* structures were considered as possible candidates for the solution structure. A complete search for all possible ring-puckering schemes as well as all possible side-chain rotamers was performed. This yielded four families of structures for the *SR* molecules (denoted as A, B, C, and D) and two families of structures for the *SS* molecules (called A′ and B′), with a family defined as those molecules that follow a common ring-puckering scheme but have different side-chain arrangements. In the discussion which follows only the lowest energy members of the families are presented.

Representations of the structural characteristics of the relatively low energy ring types A and B are given in Chart I, and the calculated structures for A and B are shown in Figures 5 and 6,

Table III. ^{13}C-NMR Data for **2** and **3**[a]

signal	δ, J	
	2	**3**
C(2)	32.93, J(P,C) = 30.8 Hz	32.37, J(P,C) = 38.3 Hz
C(3)	65.27, J(P,C) = 2 Hz	68.62
C(5)	54.42	57.39
C(6)	159.83	160.08
C(7,11)	131.34	130.95
C(8,10)	114.26	114.59
C(9)	126.83	126.75
OCH_3	55.19	55.29
C(14)	28.7, J(P,C) = 8.5 Hz	28.84, J(P,C) = 4 Hz
CH_3	17.93	18.72
	20.37	19.11
C(17,24)	124.38, J(P,C) = 56.8 Hz	124.6, J(P,C) = 64 Hz
	125.11, J(P,C) = 56.5 Hz	125.66, J(P,C) = 66 Hz
C(18,22,25,29)	132.61, J(P,C) = 10.7 Hz	132.21, J(P,C) = 10.7 Hz
	133.75, J(P,C) = 11.7 Hz	133.65, J(P,C) = 11.8 Hz
C(19,21,26,28)	129.77, J(P,C) = 4 Hz	129.6, J(P,C) = 5.3 Hz
	129.87, J(P,C) = 3.6 Hz	129.8, (P,C) = 5.4 Hz
C(20,27)	142.43, J(P,C) = 1.5 Hz	141.96, J(P,C) = 2.3 Hz
	142.48, J(P,C) = 1.4 Hz	142.36, J(P,C) = 2.7 Hz
C(23,30)	21.56	21.49
	21.58	

[a] Assignment via ^{13}C Dept135 and ^{1}H-^{13}C correlation (Inv).

Table IV. ^{1}H-NMR Data for **4**

	multiplicity no. of H's, δ	
	in $CDCl_3$	in d_8-Toluene-d_8
H–C(2)		d, 1H, 1.65
H–C(2,3,14)	m, 4H, 2.10–2.19	m, 3H, 2.12–2.35
H–C(5)	3, 4.13	m, 3.68
	d, 4.70	m, 5.77
H–C(7,11)	*a*	m, 8.22
H–C(8,10)	m, 6.77	m, 6.67
OCH_3	s, 3.77	s, 3.34
CH_3	d, 0.74	d, 0.58
	d, 0.81	d, 1.21
H–C(18,22,25,29)	m, 6H, 7.68–7.79	m, 7.85–8.05
H–C(19,21,26,28)	m, 7.0	m, 6.83
	m, 7.2	m, 6.89
H–C(23,30)	s, 2.26	s, 2.04
	s, 2.38	s, 2.09

[a] Together with H–C(18,22,25,29).

(25) Pregosin, P. S. *Phosphorus-31 NMR Spectroscopy in Stereochemical Analysis*; VCH Publishers: New York, 1987; Vol. 8, p 465.
(26) Pidcock, A.; Allen, F. H. *J. Chem. Soc. A* **1968**, 2700. Hitchcock, P.; Jacobson, B.; Pidcock, A. *J. Chem. Soc., Dalton Trans.* **1977**, 2043.
(27) Adams, D. M. *Metal-Ligand and Related Vibrations*; E. Arnold: London, 1967.
(28) (a) Allinger, N. L.; Geise, H. J.; Pyckhout, W.; Paquette, L. A.; Galluci, J. C. *J. Am. Chem. Soc.* **1989**, *111*, 1106. (b) Haasnout, C. A. G.; de Leeuw, F. A. A. M.; Altona, C. *Tetrahedron* **1980**, *36*, 2783.

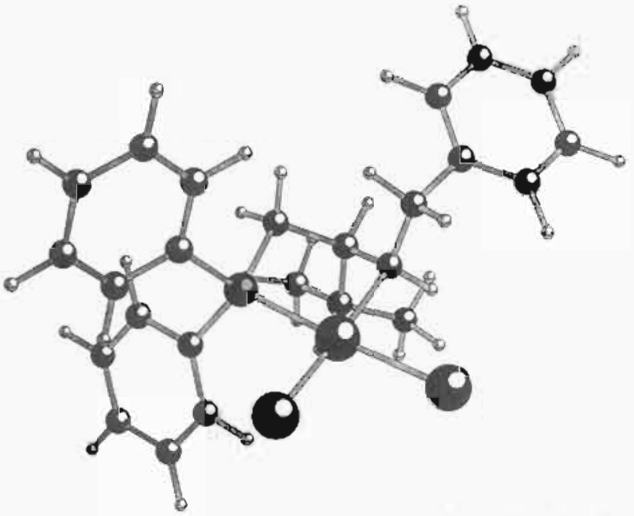

Figure 5. Calculated lowest energy structure, A, for **2**. Note that this structure contains both the C–Pr^i and N–Bz groups in pseudoaxial positions and corresponds to the solution structure.

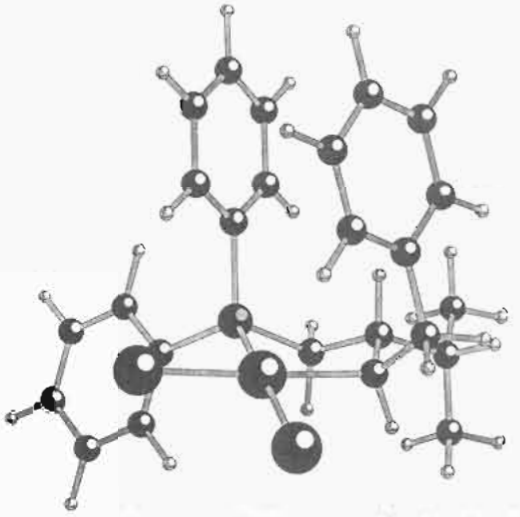

Figure 6. Calculated structure which corresponds to that found in the solid state, with pseudoequatorial substituents.

Chart I

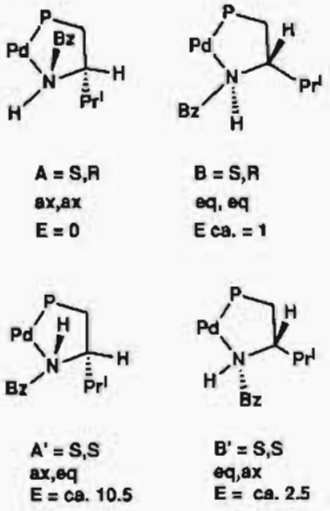

The C-3 is always S whereas the N-4 may be R or S.

The conformations within family A or B may change.

respectively. The lowest energy structure corresponds to that found in solution and has both the isopropyl group and the benzyl group roughly axial and therefore the corresponding hydrogens roughly equatorial. The next highest energy structure is type B having both the isopropyl and benzyl groups equatorial, and this arrangement is the one found in the X-ray structure. Since the energy difference between these two structures found via the calculation is only about 1 kcal/mol, it is reasonable that solvent effects (or, in the solid, packing forces) could be responsible for the preferential formation of one form and that crystallization from mixed solvents might result in a different solid-state structure. The other two structure types C and D (not shown in Chart I) show an eclipsed or nearly-eclipsed conformation with respect to the NC bond in the five-membered ring and are much higher in energy. These two structures are fairly unstable since they have the tendency to decay to A or B type structures on rotation of the side chains.

The energetic order within the families and also among families having the same stereochemistry is not very sensitive to a change in parametrization, but the energy difference between the *SS* and *SR* families is fairly sensitive to such changes. Nevertheless, the *SS* representative of lowest energy is always at higher energy than the corresponding *SR* molecule. Within the *SS* families, the structures with a relatively large P–C–C–H dihedral angle are found at high energy, whereas it is this conformation that belongs to the low-energy structures in the *SR* case, in agreement with the ^3J(P,H) data given in the solution discussion. Additional support for a solution structure of type A stems from an analysis of the dihedral angles within the ring and particularly about the CH_2CH fragment. The H–C–C–H dihedral angles in structure A are found from the calculation to be 49° and −67°. On the basis of these angles, the corresponding coupling constants are predicted[28b] to be 1.7 and 5.3 Hz, in good agreement with the ca. 1 and 6 Hz ^3J(H,H) values found experimentally. In structure type B, the two calculated angles are −62 and 178°, which should result in coupling constants of 2.3 and 12.4 Hz. With respect to the NOE contacts observed in the 2-D NOESY spectrum, we find the following distances within the lowest energy A type molecule (values for the lowest B type molecule in parentheses): (1) one Pr^i methyl group to PPh ortho protons, 3.1 Å (3.7 Å); (2) Pr^i CH proton to the same PPh ortho protons, 2.7 Å (5.5 Å); (3) other Pr^i methyl group to benzyl ortho protons, 3.7 Å (4.0 Å); (4) one of the PCH_2 protons to the NCH_2Ph protons, 2.1 Å (5.0 Å). In short, the calculations show that structure A should indeed reveal the described NOE's whereas such contacts would be very weak or zero in a structure such as B.

A picture of these relative energy considerations is given in Chart II, which represents the low-energy part of the scheme of all local minima found for the two diastereomers. The energies suggest that the *SS* molecules are present to 3.3% at most in solution. Since a change in parametrization raises the A′ and B′ energies relative to those of A and B, this estimate is likely to represent the maximum contribution of this diastereomer in solution. Since the relative energies within the *SR* molecules are much less sensitive to changes in parametrization, discussion of the energy differences between the molecules of types A and B seems on much safer ground than the comparison of the two diastereomers. The structures of family A are those that have a dihedral angle P–C–C–H of about 169°, whereas structures of type B show this angle to be 59°. If we assume a fast exchange between these two conformations (*SR*, ax, ax and *SR*, eq, eq), we can weight-average these two values by means of the relative contributions of A and B to the total population (81.4% and 15.2%, respectively). The weighted mean is about 147°, which corresponds very favorably to the rough estimate of 150° based on the NMR coupling constant. From several viewpoints, the calculations clearly support the, perhaps unexpected, difference between the solution and solid-state structures.

Chart II

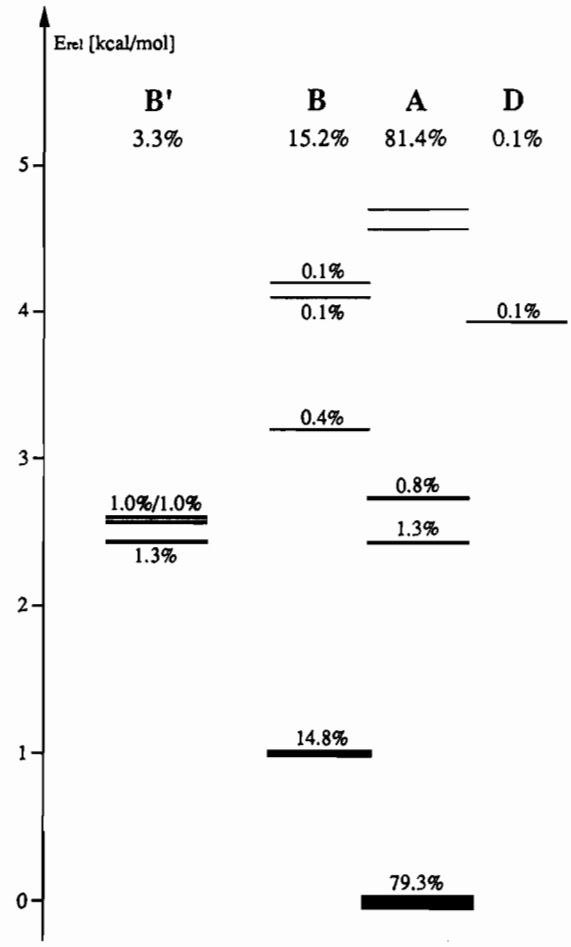

Conclusions

Viewing all of our results, we conclude the following: (a) ^{1}H NOESY methods are indeed useful in determining 3-D structures of metal complexes in solution. (b) Our complexes clearly show different solution vs solid-state structures. (c) Most importantly, the chiral pocket offered by our chelating ligand is likely to be rather flexible. Both the experiments and the calculations suggest that not much energy will be required to shift our coordinated chelate from one conformation to another, so that such complexes may well not be optimum homogeneous catalysts.

Experimental Section

Crystallography. Crystals of compound **2** were obtained by crystallization from deuteriochloroform (slow evaporation from an NMR tube) and were air stable.

Crystals suitable for the X-ray data collection were obtained with some difficulty; eventually a small, elongated prismatic crystal was found to be acceptable for data collection (even though it was scattering only weakly) and mounted on a glass fiber at a random orientation.

An Enraf-Nonius CAD 4 diffractometer was used both for the unit cell and space group determination and for the data collection. Unit cell dimensions were obtained by a least-squares fit of the 2θ values of 25 high-order reflections ($9.3 < \theta < 17.8°$) using the CAD 4 centering routines. Selected crystallographic and other relevant data are listed in Table V, while an extended list is given in supplementary Table S1.

Data were measured with variable scan speeds to ensure constant statistical precision of the collected intensities. Three standard reflections were used to check the stability of the crystal and of the experimental conditions and were measured every hour; no significant variation was detected. The orientation of the crystal was checked by measuring three other reflections every 300 measurements. Data have been corrected for Lorentz and polarization factors using the data reduction programs of the MOLEN crystallographic package.[29] An empirical absorption correction[30] was applied by using azimuthal (Ψ) scans of four "high-χ-angle" reflections ($\chi > 85.6°$; $9.0° < \theta < 16.0°$).

Table V. Experimental Data for the X-ray Diffraction Study of [**2**]·0.5$CHCl_3$

chem formula	$C_{27.5}H_{34.5}Cl_{3.5}NOPPd$
mol wt	656.563
T, °C	23
space group	$P2_12_12_1$ (No. 19)
a, Å	13.230 (4)
b, Å	17.133 (9)
c, Å	25.877 (8)
Z	8
V, Å^3	5865 (3)
ρ(calcd), g cm^{-3}	1.487
μ, cm^{-1}	8.803
λ, Å	0.710 69 (graphite monochromated, Mo K$\bar{\alpha}$)
transm coeff	0.9923–0.9006
R^a	0.062
R^b	0.064

^{a} $R = \sum||F_o| - 1/k|F_c||/\sum|F_o|$. ^{b} $R_w = [\sum w(|F_o| - 1/k|F_c|)^2/\sum w|F_o|^2]^{1/2}$ where $w = [\sigma^2(F_o)]^{-1}$ and $\sigma(F_o) = [\sigma^2(F_o^2) + f^2(F_o^2)^2]^{1/2}/2F_o$ with $f = 0.050$.

The standard deviations of the intensities were calculated in terms of statistics alone, while those of F_o were calculated as reported in Table V.

Intensities were considered as observed if $|F_o^2| \geq 2.5\sigma(F^2)$ and used for the solution and refinement of the structure. An $F_o = 0.0$ was given to those reflections having negative net intensities.

The structure was solved by a combination of direct and Fourier methods and refined by full-matrix least-squares techniques.[29] The function minimized was $[\sum w(|F_o| - 1/k|F_c|)^2])$ with $w = [\sigma^2(F_o)]^{-1}$. No extinction correction was deemed necessary.

The scattering factors used, corrected for the real and imaginary parts of the anomalous dispersion, were taken from the literature.[31] Anisotropic temperature factors were used for the palladium, phosphorus, and chlorine atoms; the remaining atoms were treated isotropically. Toward the end of the refinement, a $CDCl_3$ solvent molecule was located in a Fourier difference map and included in the refinement. This molecule is highly disordered, as can be seen from the high thermal factors and esd's; thus, only an approximate geometry has been obtained. The contribution of the hydrogen atoms in their idealized positions (C–H = 0.95 Å, $B = 5.0$ Å^2) was taken into account but not refined.

Upon convergence (no parameter shift $>0.15\sigma(p)$), the final Fourier difference map showed no significant feature. All calculations were carried out by using the Enraf-Nonius MOLEN crystallographic programs.[29]

The handedness of the crystal was tested by refining the two enantiomorphs. One of the two gave a lower R_w (at a significance level $\alpha = 0.01$); the corresponding atomic coordinates, together with the equivalent isotropic thermal factors, are given in Table VI.

Analytical Measurements. NMR spectra were recorded using Bruker AC-250, AMX-400, and AMX-500 spectrometers. Chemical shift data are in ppm, referenced to internal TMS for ^{1}H and ^{13}C and external H_3PO_4 and CH_3NO_2 for ^{31}P and ^{15}N, respectively. Two-dimensional NMR spectra (DQF-COSY, NOESY, ^{13}C-^{1}H-HMQC, and ^{15}N-^{1}H-HMQC) were measured using standard techniques for pure absorption mode representation,[33] whereas the ^{31}P-^{1}H-retro-INEPT was obtained using an adapted INEPT pulse sequence suitable for proton observation. For the NOESY measurements, mixing times between 800 and 1150 ms were generally employed.

^{31}P solid-state NMR spectra were obtained using cross-polarization (with a contact time of 2.5 ms) and magic angle spinning (at a frequency of 10 kHz) techniques. IR spectra were measured using a Perkin-Elmer 883 spectrometer. Mass spectra and microanalyses were carried out in the analytical laboratory of the ETH Zurich.

(29) *MOLEN Enraf-Nonius Structure Determination Package*; Enraf-Nonius: Delft, The Netherlands, 1990.
(30) North,. A. C. T.; Phillips, D. C.; Mathews, F. S. *Acta Crystallogr., Sect. A* **1968**, *A24*, 351.
(31) *International Tables for X-ray Crystallography*; Kynoch: Birmingham, England, 1974; Vol. IV.
(32) Hamilton, W. C. *Acta Crystallogr.* **1965**, *13*, 502.
(33) Kessler, H.; Gehrke, M.; Griesinger, C. *Angew. Chem.* **1988**, *100*, 507; *Angew. Chem., Int. Ed. Engl.* **1988**, *27*, 490 and references therein.

Table VI. Final Positional Parameters and Equivalent Thermal Factors for [2]·0.5$CHCl_3$

atom	x	y	z	B,[a] Å^2	atom	x	y	z	B,[a] Å^2
Pd(1)	0.7179 (2)	0.1165 (2)	0.9314 (1)	3.36 (6)	C(15)	0.349 (3)	0.115 (3)	0.876 (2)	7 (1)*
Pd(1′)	1.1113 (2)	−0.3701 (2)	1.0685 (1)	3.43 (6)	C(16′)	1.458 (4)	−0.211 (3)	1.127 (2)	7 (1)*
Cl(1′)	1.0029 (8)	−0.4326 (6)	1.1296 (5)	5.3 (3)	C(16)	0.370 (3)	0.254 (2)	0.851 (1)	4 (1)*
Cl(1)	0.8092 (8)	0.0159 (6)	0.8901 (5)	5.1 (3)	C(17′)	1.189 (2)	−0.218 (2)	0.995 (1)	2.6 (8)*
Cl(2′)	1.0101 (8)	−0.4022 (7)	1.0007 (5)	6.7 (4)	C(17)	0.670 (3)	0.304 (2)	0.955 (1)	2.8 (9)*
Cl(2)	0.8472 (7)	0.1313 (7)	0.9906 (4)	4.9 (3)	C(18′)	1.260 (3)	−0.168 (2)	0.973 (1)	4 (1)*
P(1)	0.6309 (8)	0.2071 (6)	0.9710 (4)	3.2 (3)	C(18)	0.600 (3)	0.359 (2)	0.940 (1)	3.8 (9)*
P(1′)	1.2171 (8)	−0.3161 (6)	1.0144 (4)	2.7 (2)	C(19′)	1.234 (2)	−0.092 (2)	0.953 (1)	3.0 (9)*
O(12′)	1.035 (2)	−0.003 (2)	1.181 (1)	6.0 (8)*	C(19)	0.636 (2)	0.433 (2)	0.929 (2)	3.3 (8)*
O(12)	0.797 (2)	0.372 (2)	0.730 (1)	6.3 (7)*	C(20′)	1.137 (2)	−0.067 (2)	0.964 (1)	3.3 (9)*
N(4)	0.590 (2)	0.122 (2)	0.880 (1)	3.3 (7)*	C(20)	0.742 (2)	0.453 (2)	0.927 (2)	3.0 (8)*
N(4′)	1.219 (2)	−0.343 (1)	1.126 (1)	2.4 (6)*	C(21′)	1.073 (2)	−0.111 (2)	0.988 (1)	1.5 (7)*
C(2′)	1.328 (3)	−0.307 (2)	1.051 (1)	4 (1)*	C(21)	0.811 (2)	0.396 (2)	0.940 (1)	3.6 (9)*
C(2)	0.505 (3)	0.193 (2)	0.943 (1)	4 (1)*	C(22′)	1.093 (3)	−0.188 (2)	1.003 (1)	3.4 (9)*
C(3′)	1.299 (3)	−0.283 (2)	1.106 (1)	3.0 (9)*	C(22)	0.775 (3)	0.323 (2)	0.957 (1)	4 (1)*
C(3)	0.526 (3)	0.184 (2)	0.885 (1)	2.9 (9)*	C(23′)	1.117 (3)	0.014 (2)	0.941 (2)	5 (1)*
C(5)	0.626 (3)	0.105 (2)	0.824 (1)	5 (1)*	C(23)	0.784 (3)	0.530 (2)	0.912 (2)	6 (1)*
C(5′)	1.177 (2)	−0.317 (2)	1.181 (1)	1.9 (8)*	C(24′)	1.246 (2)	−0.364 (2)	0.956 (1)	1.6 (7)*
C(6)	0.672 (3)	0.172 (2)	0.800 (1)	2.5 (8)*	C(24)	0.614 (3)	0.199 (2)	1.037 (1)	4 (1)*
C(6′)	1.138 (3)	−0.234 (2)	1.177 (1)	4 (1)*	C(25′)	1.288 (3)	−0.443 (2)	0.959 (1)	3.3 (9)*
C(7)	0.632 (3)	0.209 (3)	0.756 (2)	7 (1)*	C(25)	0.598 (4)	0.261 (3)	1.068 (2)	9 (1)*
C(7′)	1.058 (3)	−0.209 (2)	1.146 (1)	2.4 (8)*	C(26)	0.586 (3)	0.253 (2)	1.123 (2)	6 (1)*
C(8)	0.666 (3)	0.273 (2)	0.728 (1)	5 (1)*	C(26′)	1.307 (3)	−0.487 (2)	0.912 (1)	4 (1)*
C(8′)	1.027 (2)	−0.140 (2)	1.147 (1)	3.0 (9)*	C(27′)	1.277 (3)	−0.456 (2)	0.868 (2)	5 (1)*
C(9)	0.753 (3)	0.312 (3)	0.749 (2)	6 (1)*	C(27)	0.586 (3)	0.180 (2)	1.144 (2)	5 (1)*
C(9′)	1.068 (3)	−0.082 (2)	1.181 (2)	6 (1)*	C(28)	0.592 (3)	0.113 (2)	1.118 (1)	4 (1)*
C(10)	0.793 (3)	0.285 (2)	0.796 (2)	5 (1)*	C(28′)	1.242 (3)	−0.385 (2)	0.867 (1)	4.2 (9)*
C(10′)	1.142 (3)	−0.100 (2)	1.219 (1)	3.3 (9)*	C(29′)	1.220 (3)	−0.340 (2)	0.908 (1)	4 (1)*
C(11)	0.752 (3)	0.213 (2)	0.819 (1)	4 (1)*	C(29)	0.611 (3)	0.127 (2)	1.064 (2)	5.6 (9)*
C(11′)	1.173 (3)	−0.180 (2)	1.211 (1)	4 (1)*	C(30′)	1.292 (3)	−0.503 (2)	0.819 (2)	5 (1)*
C(13)	0.769 (4)	0.382 (3)	0.681 (2)	9 (1)*	C(30)	0.575 (3)	0.171 (2)	1.203 (2)	6 (1)*
C(13′)	1.085 (4)	0.055 (3)	1.215 (2)	8 (1)*	Cl(1)-s	0.487 (4)	−0.027 (3)	1.213 (2)	23 (3)*
C(14)	0.423 (3)	0.175 (2)	0.855 (2)	5 (1)*	Cl(2)-s	1.060 (4)	0.061 (3)	0.798 (2)	23 (2)*
C(14′)	1.389 (3)	−0.278 (2)	1.143 (1)	3.5 (9)*	Cl(3)-s	0.575 (4)	−0.138 (3)	1.255 (2)	24 (3)*
C(15′)	1.450 (3)	−0.349 (2)	1.153 (2)	4 (1)*	C-s	0.563 (8)	−0.051 (6)	1.271 (4)	22 (4)*

[a] Starred values indicate that atoms were refined isotropically. Anisotropically refined atoms are given in the form of the isotropic equivalent displacement parameter defined as $(4/3)[a^2\beta(1,1) + b^2\beta(2,2) + c^2\beta(3,3)]$. The atoms C-s and Cl-s are those of the solvent molecule.

Materials. Solvents were dried before use. All of the complexes were prepared under an argon atmosphere unless otherwise indicated.

Preparation of Sodium Valinate. L-Valine (5 g, 42.5 mmol) was dissolved in 20 mL of water, and the solution was treated with an equal volume of a solution of sodium hydroxide (1.701 g, 42.5 mmol). A 10-mL portion of ethanol was then added, and the suspension was stirred until all the solids dissolved. The solvents were then removed in vacuo, and the crude solid was used for the following reaction.

Sodium Salt of *N*-(4′-Methoxybenzylidene)-L-2-amino-3-butanoic Acid. To a 100-mL vessel were added sodium valinate (5.423 g, 38.9 mmol), anisaldehyde (5.306 g, 38.9 mmol), 40 mL of pentane, and 10 mL of ethanol, and the resulting suspension was heated under reflux for 8 h in a Dean-Stark trap. The white solid which resulted was filtered off, washed thoroughly with pentane and ether, dried, and then used without further purification (9.630 g, 96%). ^{1}H-NMR (250.13 MHz, CD_3OD): 0.91 (d, CH_3); 1.03 (d, CH_3); 2.34 (m, $CH(CH_3)_2$); 3.45 (d, H–C(2)); 7.0 (d, H–C(3′,5′)); 7.79 (d, H–C(2′,6′)); 8.23 (s, H–C(7′)).

Preparation of *N*-(4-Methoxybenzyl)-L-2-amino-3-methyl-1-butanol. To a suspension of $LiAlH_4$ (2.8 g, 74.8 mmol) in ether was slowly added the sodium salt of the Schiff base (9.6 g, 37.3 mmol) as a solid. Stirring for 30 min was followed by refluxing for 2 h. Cooling to 273 K was followed by destruction of the excess $LiAlH_4$ with water. The two phases were separated, and the water phase was washed with ether. The combined ether layers were dried over KOH, and then the ether was removed by distillation. The crude product, 6.8 g (81%), was used directly, although it can be purified by conversion to the hydrochloride followed by recrystallization from ethanol/ether. $[\alpha]_D = 10.6 \pm 1°$ ($c = 1.1$, $CHCl_3$). Anal. Calcd for $C_{13}H_{21}NO_2$ (mol wt 223.32): C, 69.92; H, 9.48; N, 6.27. Found: C, 69.81; H, 9.57; N, 6.01. ^{1}H-NMR (250.13 MHz, $CDCl_3$): 0.90 (d, CH_3); 0.96 (d, CH_3); 1.86 (m, $CH(CH_3)_2$); 2.45 (m, H–C(2)); 3.35 (m, H–C(1)); 3.62 (m, H–C(1)); 3.72 (d, H–C(7′)); 3.79 (m, OCH_3); 6.86 (m, H–C(2′,6′)); 7.24 (m, H–C(3′,5′)). ^{13}C-NMR (50.32 MHz, $CDCl_3$): 18.46, 19.54 (CH_3); 28.80 (C(3)); 50.88 (C(7′)); 55.24 (OCH_3); 60.48 (C(1)); 63.75 (C(2)); 113.87 (C(2′,6′)); 129.35 (C(3′,5′)); 132.63 (C(4′)); 158.73 (C(1′)).

Preparation of 1-Chloro-*N*-(4′-methoxybenzyl)-L-2-amino-3-methylbutane Hydrochloride. The crude *N*-(4′-methoxybenzylidene)-L-2-amino-3-methyl-1-butanol (5.67 g, 25.4 mmol) was dissolved in 30 mL of $CHCl_3$, and the solution was treated dropwise with 14 mL of thionyl chloride (23.16 g, 194 mmol) at 273 K. Stirring at this temperature was continued for 30 min, and then the temperature was raised to 333 K for 2 h. After the mixture was cooled to room temperature, the solvents and excess thionyl chloride were removed using a rotary evaporator. The reddish solid which remained was dried overnight in vacuo and then recrystallized from ethanol/ether at ca. 253 K to afford 5.26 g (74%) of product. Anal. Calcd for $C_{13}H_{21}NOCl_2$ (mol wt 278.22): C, 56.12; H, 7.61; N, 5.03. Found: C, 56.09; H, 7.66; N, 4.81. ^{1}H-NMR (250.13 MHz, $CDCl_3$): 1.06 (m, CH_3); 2.26 (m, H–C(3)); 3.03 (m, H–C(2)); 3.74 (s, OCH_3); 3.82 (m, H–C(1)); 4.06 (m, H–C(1)); 4.24 (m, H–C(7′)); 6.89 (m, H–C(3′,5′)); 7.63 (m, H–C(3′,5′)); 9.41, 10.21 (NH_2^+, broad signal). ^{13}C-NMR (50.32 MHz, $CDCl_3$): 18.16 (CH_3); 18.21 (CH_3); 29.10 (C(3)); 41.44 (C(1)); 49.29 (C(7′)); 55.28 (OCH_3); 61.89 (C(2)); 114.45 (C(3′,5′)); 121.92 (C(4′)); 132.46 (C(2′,6′)); 160.43 (C(1′)).

Preparation of 1-(Di-*p*-tolylphosphino)-*N*-(4′-Methoxybenzyl)-L-2-amino-3-methylbutane (1). A 150-mL quantity of liquid NH_3 was condensed into a three-necked flask at 195 K. Sodium metal (0.728 g, 31.7 mmol) was added, in small pieces, to afford a blue solution under argon. Addition of P(*p*-Tol)$_3$ (4.381 g, 14.39 mmol) was followed by stirring for 2 h. The resulting red solution was then treated with 1-chloro-*N*-(4′-methoxybenzyl)-L-2-amino-3-methylbutane hydrochloride (4.00 g, 14.39 mmol). The resulting suspension was stirred overnight, during which time the NH_3 was allowed to evaporate. The white mass which remained was extracted with hexane. Removal of the hexane afforded the crude product as a colorless air-sensitive oil, 5.56 g (92%), which could be used directly in the preparation of the complexes. This material can be purified via solution in ether, under argon, and by treatment with gaseous HCl to afford the hydrochloride, which is not ether soluble. This latter compound can be recrystallized from ethanol/hexane and the phosphine–amine complex regenerated via deprotonation using NaOH; however, the yield starting from the chloride is now ca. 38%. Data for the purified product are as follows. Anal. Calcd for $C_{27}H_{34}NOP$ (mol wt 419.55): C, 77.30; H, 8.17; N, 3.34. Found: C, 76.49; H, 7.79; N, 3.51. ^{31}P-NMR (101.27 MHz, $CDCl_3$): −24.58. ^{1}H-NMR (250.13 MHz, $CDCl_3$): 0.87 (m, CH_3); 2.02 (m, 2H, H–C(2), H–C(14)); 2.22

(m, H–C(2)); 2.24, 2.34 (6H, H–C(23,30)); 2.43 (m, H–C(3)); 3.64 (s, H–C(5)); 3.81 (s, OCH_3); 6.80 (m, H–C(8,10)); 7.13 (m, 6H, H–C(7,11), H–C(19,21,26,28)); 7.32 (m, 4H, H–C(18,22,25,29)). ^{13}C-NMR (50.32 MHz, $CDCl_3$): 17.29, 18.40 (CH_3); 21.33, 21.37 (C(23,30)); 30.18 (C(14), J(P,C) = 7.45 Hz); 30.48 (C(2), J(P,C) = 12.3 Hz); 51.11 (C(5)); 55.29 (OCH_3); 59.36 (C(3), J(P,C) = 12.6 Hz); 113.65 (C(8,10)); 129.2–129.5, 132.36–133.9 (arom C–H); 134.15–138.65 (arom quat C); 158.46 (C(6)). $[\alpha]^{25}_D$ = 52.6 ± 1° (c = 0.68, $CHCl_3$).

Alternative Preparation of *N*-(4′-Methoxybenzylidene)-L-2-amino-3-methyl-1-butanol. L-Valinol (0.931 g, 9.02 mmol) was dissolved in 60 mL of toluene. Anisaldehyde (1.228 g = 1.09 mL, 9.02 mmol) was added using a syringe. Heating for 3 h at 60 °C in a Dean-Stark trap under 200-mbar pressure in the presence of $MgSO_4$ was followed by removal of the solvent in vacuo. The oil which resulted was recrystallized from hexane to afford the product, 1.455 g (73%). ^{1}H-NMR (250.13 MHz, $CDCl_3$): 0.85 (d, CH_3); 0.94 (d, CH_3); 1.05 (*CH_3); 1.63 (m, H–*C(3)); 1.92 (m, H–C(3)); 2.91 (m, H–C(2)); 3.13 (m, H–*C(2)); 7.38 (m, H–C(3′,5′), H–*C(3′,5′)); 7.38 (m, H–*C(2′,6′)); 7.62 (m, H–C(2′,6′)); 7.81 (s, H–C(7′)). Note: *C indicates ring-closed isomer.

Alternative Preparation of *N*-(4′-Methoxybenzyl)-L-2-amino-3-methyl-1-butanol. A 100-mg quantity of 5% Pd/charcoal was added to a flask containing 50 mL of methanol and the vessel flushed three times with hydrogen. *N*-(4′-Methoxybenzylidene)-L-2-amino-3-methyl-1-butanol (1.456 g, 0.658 mmol) in 20 mL of methanol was added and the suspension stirred overnight. Filtration followed by removal of the solvent afforded the crude product (1.171 g, 0.524 mmol). A 0.2-g sample of this material was dissolved in ether, and the solution was treated with HCl gas for 10 min. The insoluble salt which precipitated was collected by filtration and then recrystallized from ethanol/ether. Deprotonation with 1 M NaOH in ether followed by the usual workup, as above, gave the product as a yellowish oil in 80% yield.

Preparation of 2. $PdCl_2(CH_3CN)_2$ (0.118 g, 0.427 mmol) was suspended in 20 mL of toluene, the suspension was warmed until the solid dissolved, and the resulting solution was treated with **1** (0.1792 g, 0.427 mmol). Stirring for 30 min was followed by filtration through Celite. Removal of the solvent and recrystallization using CH_2Cl_2/ether afforded 160.3 mg (63 %) of product. Anal. Calcd for $C_{27}H_{34}NOPCl_2Pd$ (mol wt 596.57): C, 54.33; H, 5.74; N, 2.35. Found: C, 53.91; H, 5.81; N, 2.38. ^{31}P-NMR (101.27 MHz, $CDCl_3$): 45.1. ^{31}P-NMR (161.98 MHz, solid state): 45.3, 49.7. ^{15}N-NMR (40.55 MHz, $CDCl_3$): –321.6 (J(N,H) = 71.7 Hz). IR (CsI): ν(N–H) = 3111 cm^{-1}, ν(Pd–Cl) = 332, 270 cm^{-1}. $[\alpha]_D$ = –86.0 ± 1° (c = 1, $CHCl_3$). FAB: 562.0; 524.0; 418.1, 318.9; 213.0; 121.0; 90.9.

Preparation of 3. Zeise's salt (0.236 g, 0.640 mmol) was dissolved in a minimum of warm ethanol. To this was then added **1** (0.269 g, 0.640 mmol) in ca. 5 mL of CH_2Cl_2. Stirring for 30 min was accompanied by precipitation of a white solid. Filtration to remove the solid KCl was followed by removal of the solvent to afford a solid which was again dissolved in CH_2Cl_2; the resulting solution was filtered to remove further KCl. After removal of solvent, the product (0.303 g, 72%) was obtained via recrystallization from (a minimum amount of) CH_2Cl_2/ether. Anal. Calcd for $C_{27}H_{34}NOPCl_2Pt$ (mol wt 685.53): C, 47.31; H, 5.00; N, 2.04. Found: C, 47.12; H, 5.04; N, 1.99. ^{31}P-NMR (101.27 MHz, $CDCl_3$): 16.9 (J(Pt,P) = 4040.4 Hz). ^{31}P-NMR (161.98 MHz, solid state): 18.0 (J(Pt,P) = 3914 Hz). ^{15}N-NMR (40.55 MHz, $CDCl_3$): –330.4 (J(N,H) = 73.3 Hz). IR (CsI): ν(N–H) = 3263 cm^{-1}, ν(Pt–Cl) = 331, 288 cm^{-1}. $[\alpha]_D$ = –58.6 ± 1° (c = 1, $CHCl_3$). FAB: 650.0; 611.0; 484.5; 314.5; 121.0; 90.9.

Preparation of 4. Complex **3** (0.100 g, 0.145 mmol) under argon was dissolved in 3 mL of CH_2Cl_2, and the solution was treated with solid $NaOBu^t$ (15.43 mg, 0.16 mmol). The resulting mixture was stirred for 30 min and then filtered to remove NaCl. Removal of solvent was followed by recrystallization from (a minimum of) CH_2Cl_2/ether to give 93 mg (99%) of product. Anal. Calcd for $[PtCl(\mathbf{1} - H)]_2 \cdot 2H_2O$, $C_{54}H_{70}Cl_2O_4N_2P_2Pt_2O_2$ (mol wt 1334.14): C, 48.59; H, 5.24; N, 2.10. Found: C, 47.90; H, 5.24; N, 2.06. X-ray fluorescence (Siemens SR-1): [Cl]/[Pt] 0.97 ± 0.05; [P]/[Pt] = 0.97 ± 0.03. ^{31}P-NMR (101.27 MHz, $CDCl_3$): 10.0 (J(Pt,P) = 3628.3 Hz). ^{31}P-NMR (101.27 MHz, toluene-d_8): 10.9 (J(Pt,P) = 3693.6 Hz). ^{13}C-NMR (62.89 MHz, $CDCl_3$; sample preparation involved filtering $CDCl_3$ twice through basic Alox): 17.14 (CH_3); 21.40 (CH_3); 21.50 (C(23,30)); 26.41 (C(14), J(P,C) = 10.3 Hz); 31.06 (C(2), J(P,C) = 38.3 Hz); 52.17 (C(5)); 55.16 (OCH_3); 65.99 (C(3)); 113.67 (C(8,10)); 124.60, 125.60 (C(17), C(24)); 129.16–129.42 (m, C(19,21,26,28)); 131.67 (C(7,10)); 133.12–133.38 (m, C(18,22,25,29)); 140.89, 141.37 (C(20), C(28)); 159.26 (C(6)). FAB: 1316.1, 1298; 1133.1; 1056.1; 912.2; 835.0; 801.0; 752.1; 705.2; 650.0; 485.9; 315.9; 281.0; 207.0; 154.0; 121.0; 72.9.

Reaction of 4 in $CDCl_3$. A 0.9-mL portion of $CDCl_3$ was filtered twice through basic Alox, and this solvent was used to dissolve 40 mg (0.031 mmol) of 4. The NMR tube was then degassed and sealed. ^{31}P-NMR (101.27 MHz): 10 (J(P,Pt) = 3628 Hz). In the ^{31}P-NMR spectrum after 1 day the following were observed:

signal 1	10.2 ppm, J(Pt,P) = 3625 Hz	spectrum of **4**
signal 2	11.2 ppm, J(Pt,P) = 4057 Hz	
signal 3	16.9 ppm, J(Pt,P) = 4038 Hz	spectrum of **3**

After 3 days, the ^{31}P-NMR spectrum shows only **3** (16.9 ppm, J(P,Pt) = 4036 Hz) and the ^{1}H-NMR spectrum shows only the resonances for **3**, without the NH signal.

Preparation of 5. Complex **3** (0.050 g, 0.073 mmol) was dissolved in 15 mL of acetone, and the solution was treated with NaI (0.0229 g, 0.153 mmol). The mixture was stirred for 1 h. Removal of the solvent was followed by dissolving the resulting solid in CH_2Cl_2, filtration to remove the NaCl, removal of the solvent again, and recrystallization using CH_2Cl_2/ether to afford 43.4 mg (69%) of the yellow product. ^{1}H-NMR (250.13 MHz, $CDCl_3$): 0.49, 0.72 (d, CH_3); 2.04 (m, H–C(14)); 2.17–2.43 (m, 3H, H–C(2), H–C(3)); 2.38 (s, 6H, H–C(23,30)); 3.56 (q, 1H, H–C(5)); 3.80 (OCH_3); 4.99 (m, 2H, NH, H–C(5)); 6.88 (m, H–C(8,10)); 7.24 (m, H–C(19,21,26,28); 7.35 (m, H–C(7,11)); 7.77, 7.97 (m, H–C(18,22,25,29)). ^{31}P-NMR (101.27 MHz, $CDCl_3$): 18.7 (J(Pt,P) = 3842 Hz).

Acknowledgment. P.S.P. thanks the Swiss National Science Foundation and the ETH Zurich for financial support, as well as Johnson Matthey for the loan of precious metals. A.A. thanks the Italian CNR for a grant.

Supplementary Material Available: An extended list of experimental parameters (Table S1), a list of calculated positional parameters for the hydrogen atoms (Table S2), a list of anisotropic displacement parameters (Table S3), extended lists of bond distances and bond angles (Tables S4 and S5), and a list of torsion angles (Table S6) (14 pages). Ordering information is given on any current masthead page.